

Freier Zugang | Veröffentlicht: 03. April 2017

Chitosan fördert die Krebsprogression und Stammzeleigenschaften in Verbindung mit der Wnt-Signalgebung in Dickdarm- und hepatozellulären Karzinomzellen

[Po-Hsiang Chang](#), [Keisuke Sekine](#), [Hsiao-Mei Chao](#), [Shan-hui Hsu](#)  & [Edward Chern](#) 

[Wissenschaftliche Berichte](#) **7**, Artikelnummer: 45751 (2017)

7124 Zugriffe | **34** Zitate | **261** Altmetric | [Metrik](#)

Abstrakt

Krebsstammzellen (CSCs), eine kleine Population von Krebszellen, gelten als Ursprung der Krebsentstehung, des Wiederauftretens und der Metastasierung. Die Tumormikroumgebung liefert entscheidende Signale für CSCs, um die Stammzeleigenschaften zu erhalten, und fördert die Tumorgenese. Daher ist die Etablierung eines geeigneten Zellkultursystems zur Nachahmung der Mikroumgebung für CSC-Studien ein wichtiges Thema. In dieser Studie züchteten wir Dickdarm- und hepatozelluläre Karzinomzellen (HCC) auf Chitosanmembranen und bewerteten die Tumorprogression und die CSC-Eigenschaften. Experimentelle Ergebnisse zeigten, dass die Kultivierung von Krebszellen auf Chitosan die Zellmotilität, die Arzneimittelresistenz, die Ruhepopulation, die Selbsterneuerungskapazität und die Expressionsniveaus von Stamm- und CSC-Markergenen wie OCT4, NANOG, CD133, CD44 und EpCAM erhöhte. Darüber hinaus haben wir gezeigt, dass Chitosan die kanonische Wnt/ β -Catenin-CD44-Achsen-signalisierung in CD44^{Positiv} Darmkrebszellen und nicht-kanonische Wnt-STAT3-Signalisierung in CD44^{Negativ} HCC-

Chitosan-Kultursystem bietet eine komfortable Plattform für die Erforschung der CSC-Biologie und das Screening von Krebsmedikamenten.

Einleitung

Krebs ist eine der häufigsten Todesursachen weltweit und wird mit Mortalität und Morbidität in Verbindung gebracht¹. Die gängigen Krebstherapien wie Strahlentherapie und Chemotherapie können zu Arzneimittelresistenzen und weiteren nachfolgenden Krebsrezidiven oder Metastasen führen. Neue Beweise deuten darauf hin, dass bestimmte Subpopulationen von Krebszellen in einem Tumor der Ursprung des Tumors sein könnten. Sie teilen einige ähnliche Eigenschaften mit Stammzellen und werden als Krebsstammzellen (CSCs) bezeichnet.^{2,3} Diese Zellen besitzen eine höhere Migrationsfähigkeit, die mit Invasion und Metastasierung verbunden ist⁴. Sie bleiben auch in einem langsamen / ruhenden Zustand, um Antiproliferationsmedikamenten zu widerstehen⁵. CSCs exprimieren spezifische Oberflächenmarker wie CD133, EpCAM und CD44, die zur CSC-Identifizierung und -Isolierung verwendet werden⁶. CSCs können sich selbst erneuern, um CSC-Pools zu erhalten und sich in heterogene Krebszellen zu differenzieren⁷. Signalkaskaden innerhalb von CSCs wie Notch, STAT3 und Wnt/ β -Catenin sind fehlreguliert, um ihre Stammzeleigenschaften zu erhalten⁸. Bei Darmkrebs ist Wnt / β -Catenin essentiell, um die CSC-Population zu erhalten. Stimulation des Wnt/ β -Catenin-Signalwegs auf differenzierten Darmkrebszellen kann CSC-Eigenschaften wiederherstellen⁹. Der nichtkanonische Wnt5-Frizzled2-Signalweg reguliert auch den epithelial-mesenchymalen Übergang (EMT), ein Merkmal von CSCs, und fördert die Metastasierung in hepatozellulären Karzinomen (HCC) und Darmkrebszellen durch die Aktivierung von STAT3¹⁰. Das phosphorylierte STAT3 wird in CSCs beobachtet, um die Stammeigenschaften hochzuregulieren¹¹. Das Targeting von CSCs und der spezifischen essentiellen Signalübertragung kann neue therapeutische Strategien liefern¹². Aufgrund der Knappheit von CSCs innerhalb der Tumoren² ist die

In Tumormikroumgebungen unterstützen extrazelluläre Matrix (ECM) und Stromazellen die Krebsentstehung und -stammung¹³. Neuere Studien haben gezeigt, dass einige biokompatible Materialien tumorassoziierte EZM nachahmen können¹⁴. Einige Gruppen haben die Biomaterialien verwendet, um dreidimensionale (3D) Gerüste zur Kultivierung von Krebszellen herzustellen.^{15,16} Zum Beispiel zeigten Eierstockkrebszellen, die in Gelatine-Methacrylamid-Hydrogele eingebettet waren, eine höhere Arzneimittelresistenz¹⁷. Ewing-Sarkomzellen in porösen elektrogesponnenen Polycaprolacton-Gerüsten zeigten die Expressionssignalmuster, die Tumoren *in vivo* ähneln¹⁸. Darüber hinaus zeigten frühere Studien, dass Crosstalks zwischen CSCs und der Mikroumgebung die Eigenschaften von CSCs aufrechterhalten könnten.^{19,20} Chang *et al.* zeigte, dass die Laminin 511-Matrix, eine Art von ECM, die CSC-Eigenschaften der Brust unterstützt und beibehält.²¹ Daher ist die Etablierung einer einfachen Biomaterialplattform zur Kultivierung von Krebszellen ein wesentlicher Schritt zur Untersuchung der Krebsstammungsbildung.

Chitosan ist ein kationisches natürliches Polysaccharid, das aus Chitin gewonnen wird und aufgrund seiner antibakteriellen Aktivität, Biokompatibilität und biologischen Abbaubarkeit in vielen biomedizinischen Bereichen eingesetzt wird²². Chitosan vernetzt mit anderen Molekülen wurde auch verwendet, um Krebszellen zu kultivieren^{23,24}. Zum Beispiel können poröse Chitosan-Alginat-Gerüste die CD133-Glioblastom-CSC-Population anreichern.²⁵ and electrospun polycaprolactone-chitosan scaffolds may increase the breast cancer stemness²⁶. However, the mechanisms of interactions between cells and biomaterials are still unknown. Our previous study showed that chitosan (CS) membranes and hyaluronan (HA) grafted chitosan (CSHA) membranes could increase the stemness of mesenchymal stem cells (MSCs)²⁷. HA is the principal ligand of receptor CD44 that is aberrantly expressed on the surface of CSCs²⁸. CSHA membranes promoted the aggressiveness of lung cancer cells possibly via the interaction of HA with CD44 receptor²⁹. Yet, the influence of chitosan itself on cancer cells remains to be elucidated.

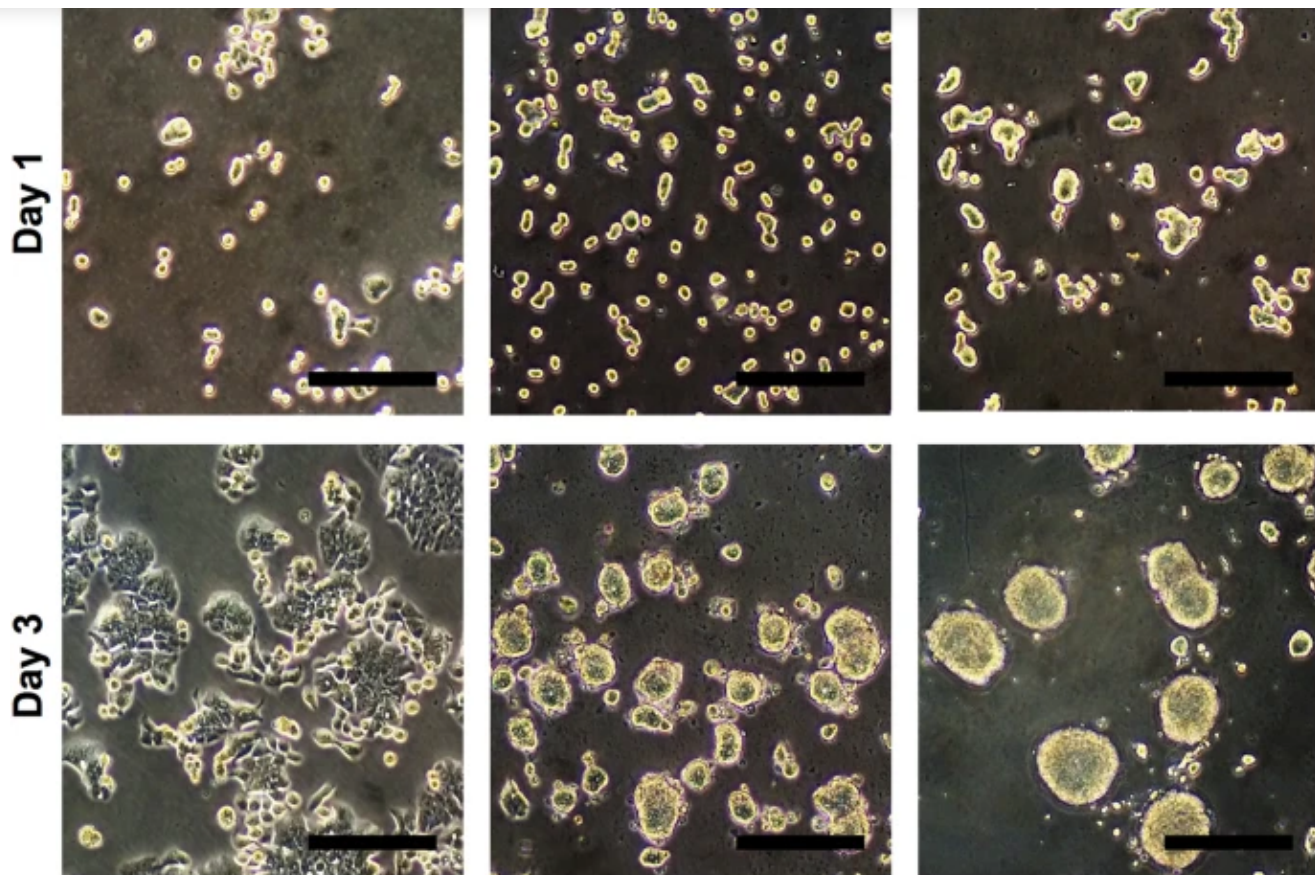
chemical properties of chitosan might resemble HA to some extent. Here, we attempted to clarify the effect of chitosan without any surface modification on colon cancer cells and HCC cells. We showed that chitosan itself promoted CSC-related characteristics and tumor progression of not only CD44^{positive} colon cancer cells but also CD44^{negative} HCC cells. We unraveled the mechanisms regarding how chitosan substrates promoted cancer stemness and revealed that canonical and noncanonical Wnt signaling pathways played key roles in the interactions between chitosan and cancer cells. Chitosan as culture substrates may provide a convenient platform that mimics ECM for the research of CSC biology and drug screening.

Results

Morphologies of colon cancer and HCC cell lines on CS and CSHA membranes

To investigate how CS and CSHA membranes directly affect the phenotypes of colon cancer cell lines HT29, DLD-1, HCT116, SW480 and HCC cell lines Huh7, HepG2, Hep3B, SKHep-1, we cultured the cells on membranes for 72 hrs following observation per 24 hrs. All cell lines attached on tissue culture polystyrene (TCP) plates and demonstrated the normal epithelial phenotype, but cells cultured on CS and CSHA membranes displayed different morphologies. Among colon cancer cell lines, only HT29 formed spheroids on both CS and CSHA membranes ([Fig. 1a](#), [Supplementary Fig. S1](#), [Supplementary video](#)). For HCC cell lines, most of them remained epithelial phenotypes on CS membranes but formed clusters on CSHA membranes ([Fig. 1b](#), [Supplementary Fig. S1](#), [Supplementary video](#)). Meanwhile, Huh7 aggregated into colonies on both CS and CSHA membranes.

Figure 1: Morphology of cancer cells on CS and CSHA membranes.



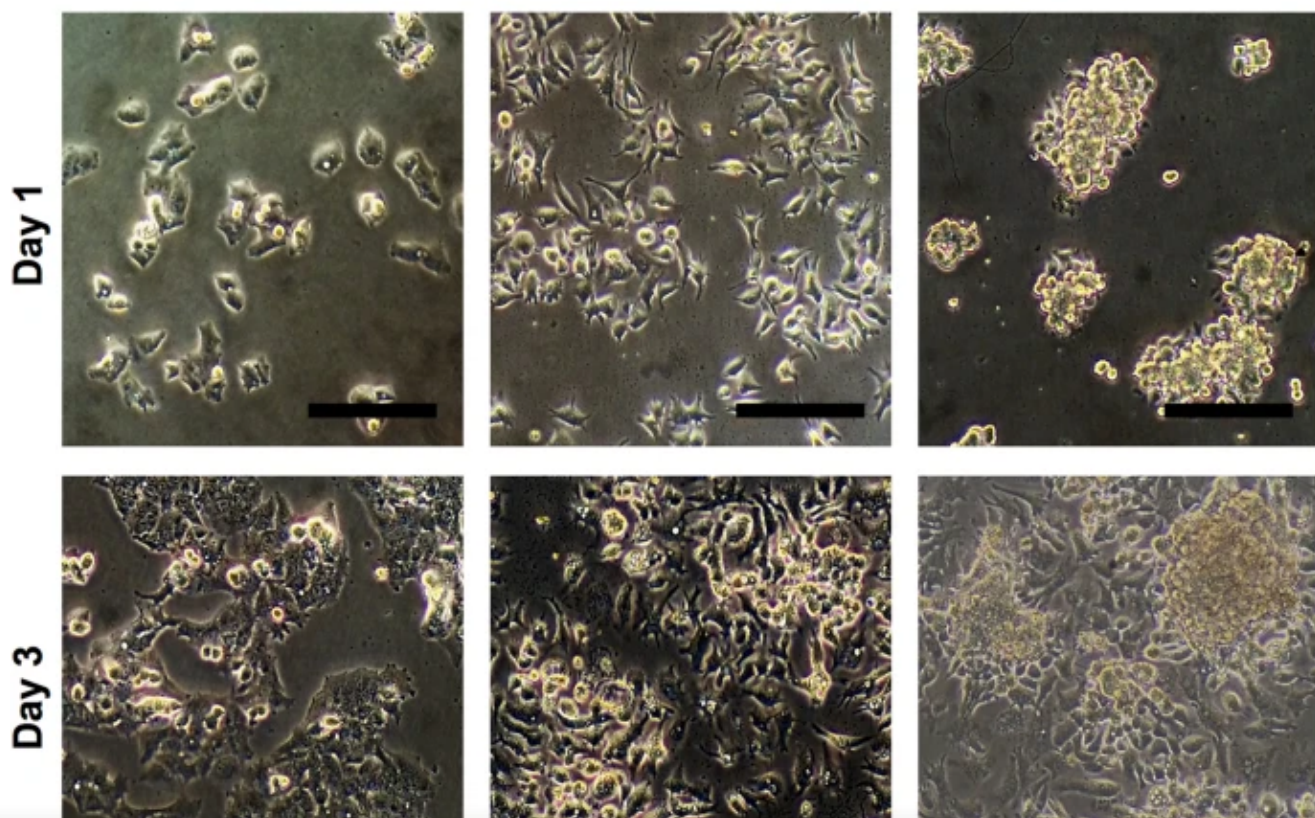
b

Huh7

TCP

CS

CSHA

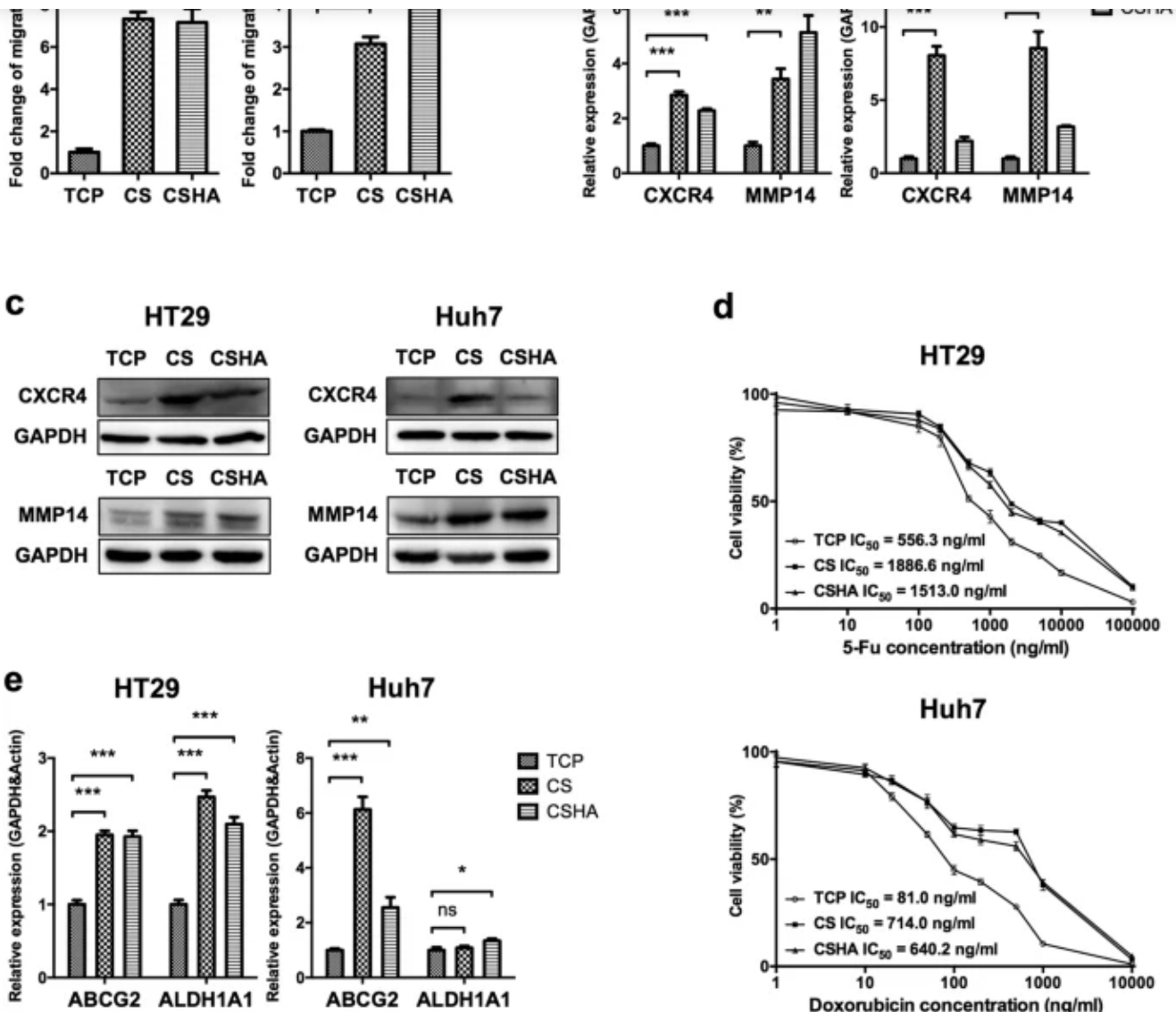


24 and 72 hrs. Scale bar represents 200 μm .

CS promoted cell motility and drug resistance

The *in vitro* transwell assay was used to examine the effect of CS and CSHA substrates on cell migration. As shown in [Fig. 2a](#), the migration ability of both HT29 and Huh7 was promoted on either CS or CSHA membranes. In addition, cells cultured on CS and CSHA membranes increased the expression of CXCR4 and MMP14 in both HT29 and Huh7 ([Fig. 2b,c](#)). Moreover, knockdown of MMP14 reduced the migration ability of both cell lines, whereas knockdown of CXCR4 only reduced the migration ability of HT29 ([Supplementary Fig. S2](#)). To understand whether cells cultured on CS and CSHA membranes increased the drug resistance, we employed two different chemotherapeutic drugs, 5-Fluorouracil and doxorubicin, to treat HT29 and Huh7 respectively. The results revealed that cells cultured on CS and CSHA membranes had higher viability than those cultured on TCP plates ([Fig. 2d](#)). Upon drug treatment, the IC_{50} values for HT29 and Huh7 grown on TCP plates were 556.3 and 81.0 ng/mL for 5-Fu and doxorubicin, respectively. The values of IC_{50} increased to 1886.6 and 714.0 ng/mL for HT29 and Huh7 on CS membranes. Similarly, the values of IC_{50} increased to 1513.0 and 640.2 ng/mL for those cells on CSHA membranes. Moreover, the expression level and enzyme activity of ALDH1A1 increased for HT29 and Huh7 cultured on CS and CSHA membranes ([Fig. 2e](#), [Supplementary Fig. S3](#)). On the other hand, the expression level and function of ABCG2 significantly increased for both HT29 and Huh7 on CS and CSHA membranes ([Fig. 2e](#), [Supplementary Fig. S4](#)).

Figure 2: Analysis of cell motility and drug resistance and associated gene expressions.

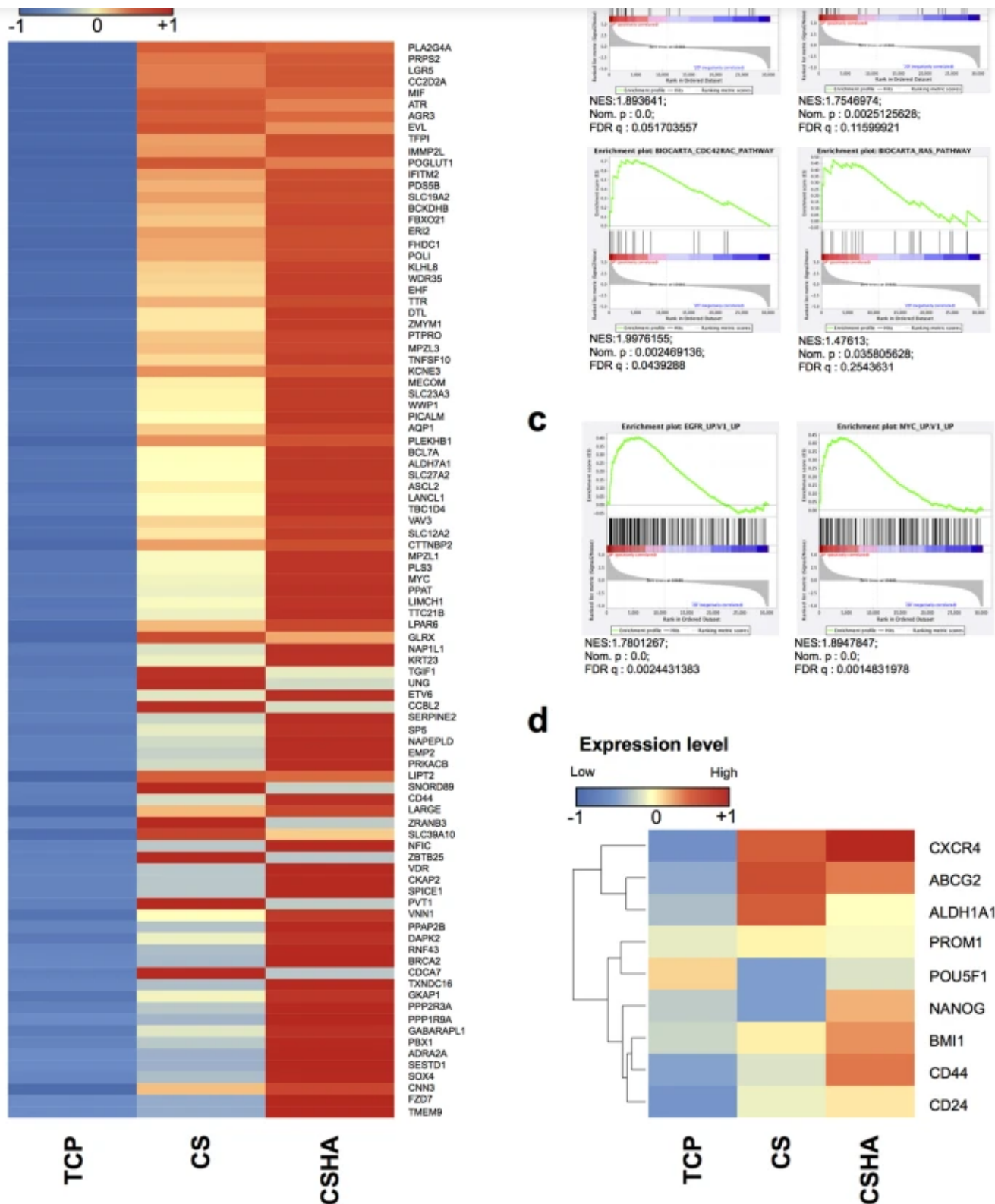


(a) The migrated cell numbers were quantified by the transwell migration assay and normalized to the TCP group. (b) CXCR4 and MMP14 mRNA expressions after 72 hrs of culture. (c) The protein expression level of CXCR4 and MMP14 after 72 hrs of culture. (d) Cell viability after treatments with varying concentrations of 5-Fu (1, 10, 100, 200, 500, 1,000, 2,000, 5,000, 10,000, and 100,000 ng/mL) and doxorubicin (1, 10, 20, 50, 100, 200, 500, 1,000, and 10,000 ng/mL) for HT29 and Huh7, respectively. Each point represents the means of six determinations (n = 6). (e) The mRNA expression levels of ABCG2 and ALDH1A1 after 72 hrs of culture. Each bar represents the means of three determinations ± SD. *p < 0.05, **p < 0.01, ***p < 0.001 among the indicated groups.

Increased stemness and cancer properties analyzed by microarray gene expression

membranes increased the expression of intestinal stem cell related genes ([Fig. 3a](#)). The results of Gene Set Enrichment Analysis (GSEA) indicated that cells on chitosan substrates increased the genes related to mTOR, eIF4, Cdc42, and Ras signaling pathways, which are associated to the cancer progression and invasiveness ([Fig. 3b](#)). CS substrates also promoted the expressions of EGFR/Myc target genes that modulate cancer proliferation ([Fig. 3c](#)). Besides, cancer stemness core genes were also upregulated in the cells cultured on the CS membranes ([Fig. 3d](#)). These transcriptome analysis data indicated that the cultivated cells on CS substrates increased the expression of genes related to stemness and cancer progression.

Figure 3: Microarray analysis of colon cancer cell line HT29 grown on TCP plates, CS, and CSHA membranes.

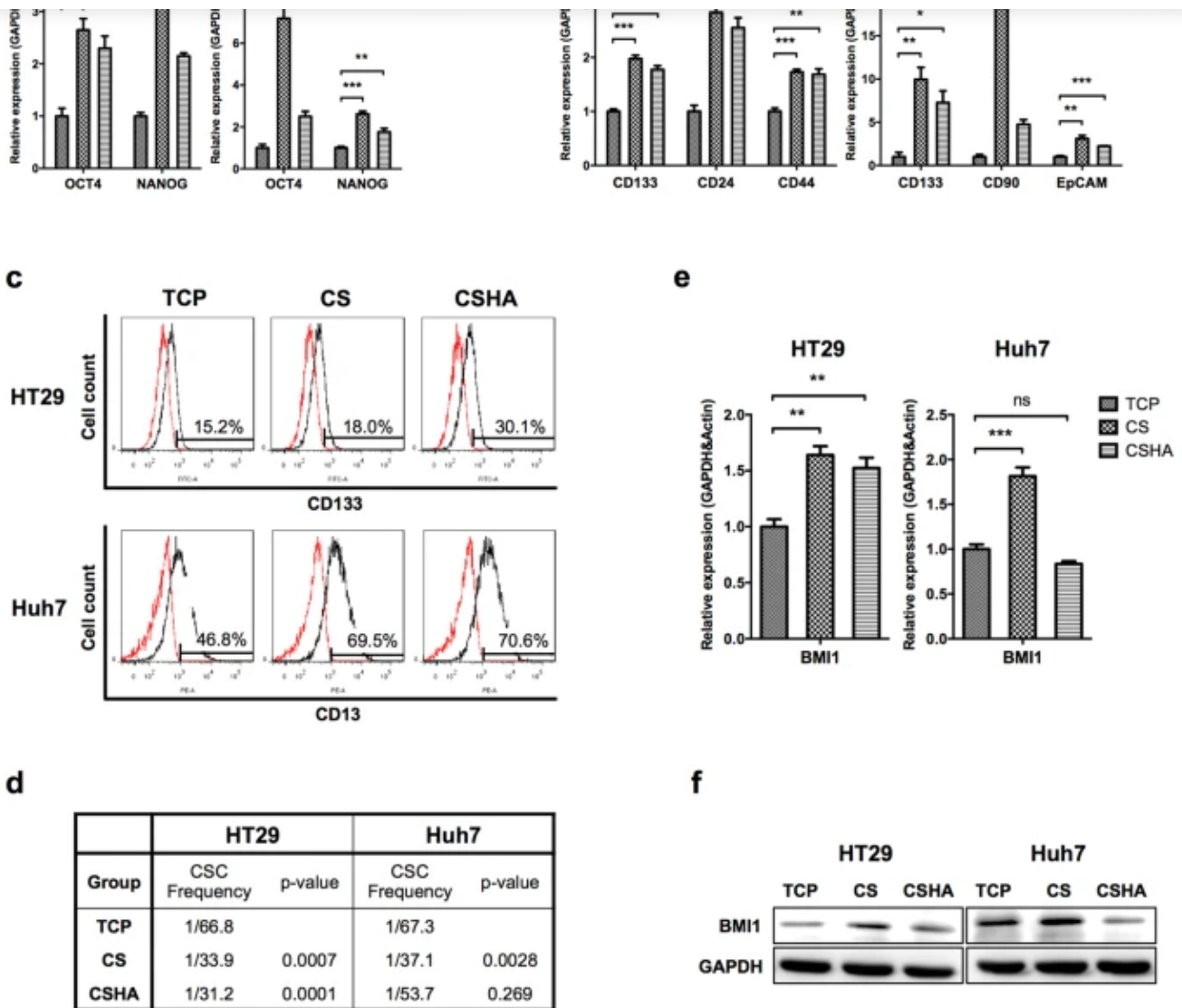


(a) Heatmap of expression levels for genes related with colon stem cells. (GEO: GSE93704)
 (b) GSEA analysis of gene set related to mTOR, eIF4, Cdc42, and Ras signaling pathways. (c) GSEA analysis of EGFR and Myc target gene set. Normalized Enrichment Score (NES), Nominal p-value (NOM.p) and FDR q-value (FDRq) were shown in the figure. (d) Heatmap of

CS increased the stemness and the population of CSCs

The stemness genes (OCT4 and NANOG) and CSC biomarkers were analyzed by RT-PCR. As shown in [Fig. 4a](#), the expression levels of OCT4 and NANOG in both HT29 and Huh7 significantly increased on CS and CSHA membranes as compared to TCP plates. The HT29 CSC markers, CD133, CD24, and CD44, were significantly upregulated on CS and CSHA membranes ([Fig. 4b](#)). The Huh7 CSC markers, CD133, CD90, and EpCAM, were also significantly upregulated on CS and CSHA membranes ([Fig. 4b](#)). The other cell lines demonstrated similar results ([Supplementary Fig. S5](#)). The gene expression of HT29 spheres from non-adherent sphere forming culture system, another 3D culture system, was also analyzed. All CS, CSHA and sphere culture systems increased stem cell properties ([Supplementary Fig. S5](#)). Moreover, we evaluated the protein levels of CSC markers, CD133 in HT29 and CD13 in Huh7. Results showed that CD133-positive cells in HT29 increased from 15.2% on TCP plates to 18.0% and 30.1% on CS and CSHA membranes, respectively. Although the mRNA level of CD13 in Huh7 was not changed on CS and CSHA membranes as compared to TCP plates, CD13-positive cells increased from 41.1% to 66.5% and 67.6%, respectively ([Fig. 4c](#)). The ELDA sphere forming assay was performed to examine the CSC frequency and self-renewal capacity. As shown in [Fig. 4d](#), the CSC frequencies on CS and CSHA membranes were significantly higher than those on TCP plates in both HT29 and Huh7. The expression level of BMI1, a transcription factor associated with self-renewal property, increased for HT29 on CS and CSHA membranes as compared to TCP plates. The BMI1 expression increased for Huh7 only on CS membranes ([Fig. 4e,f](#)). Besides, the side population assay was performed to evaluate the CSC ratios. Both side populations in HT29 and Huh7 cultured on CS and CSHA membranes elevated compared to TCP plates ([Supplementary Fig. S4](#)).

Figure 4: Evaluation of the stemness and the population of CSCs.

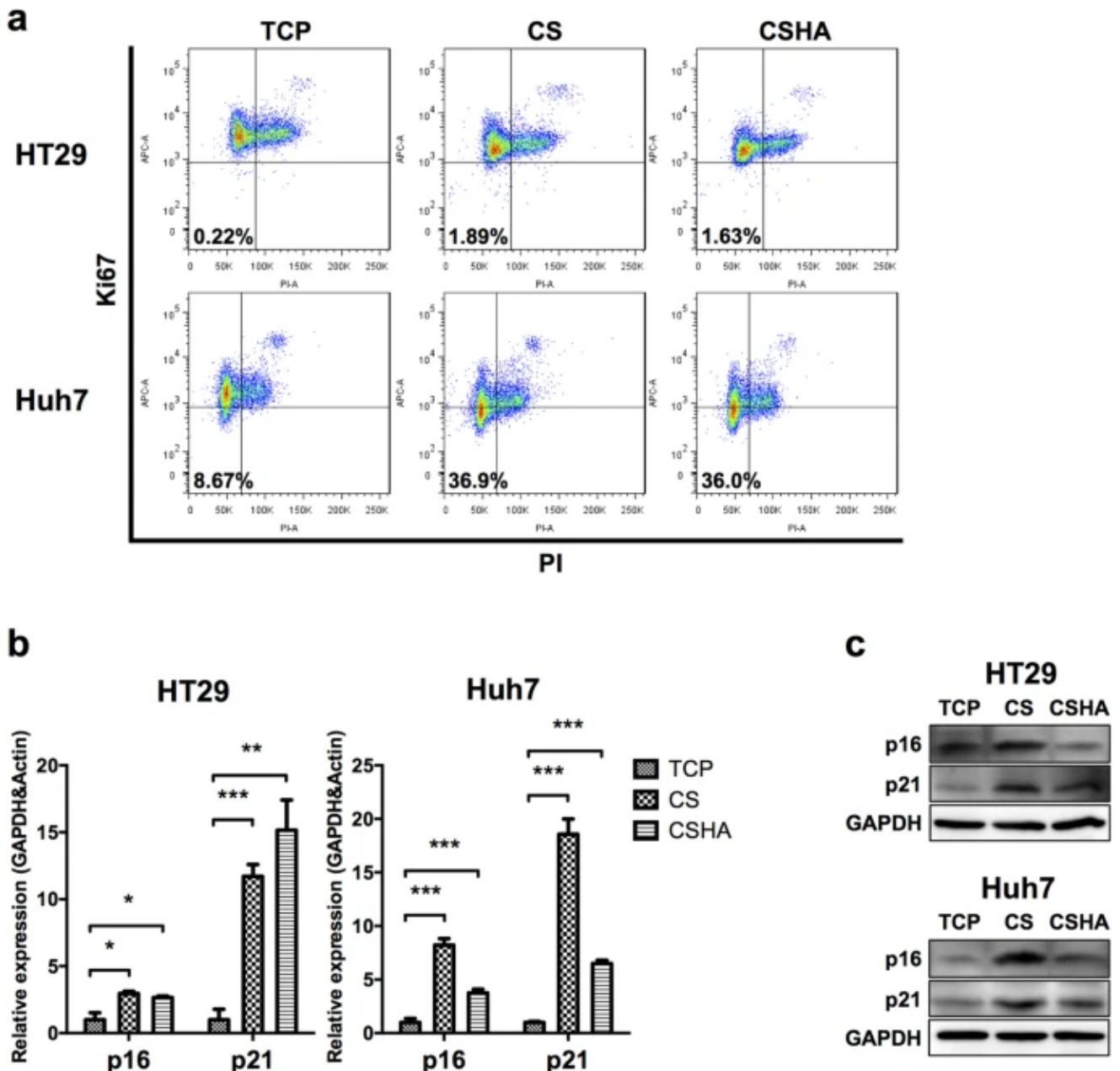


CS increased the quiescent population

Staying at quiescent state is an important property of CSCs. The quiescent population was performed using the Ki-67/PI quiescence assay. Results revealed that the

and 36.0%, respectively (Fig. 5a). The expression levels of cell cycle arrest related genes as p16 and p21 also increased on CS and CSHA membranes for both HT29 and Huh7 (Fig. 5b,c).

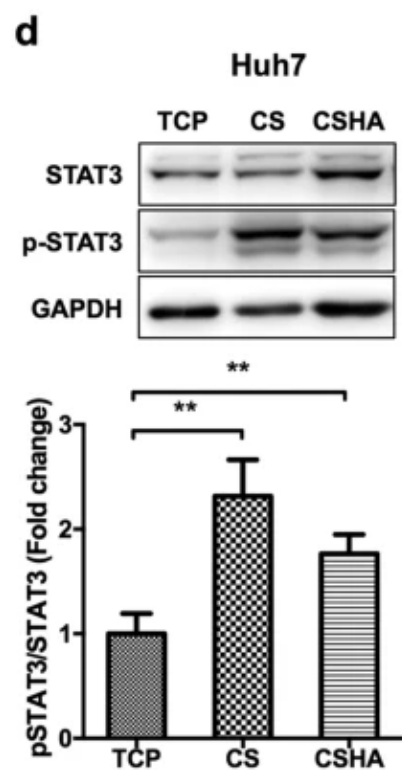
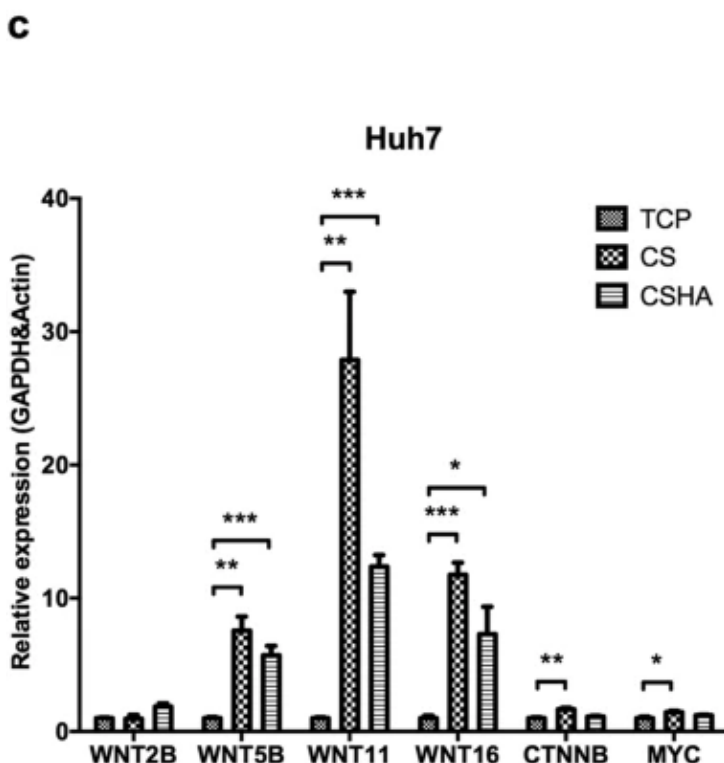
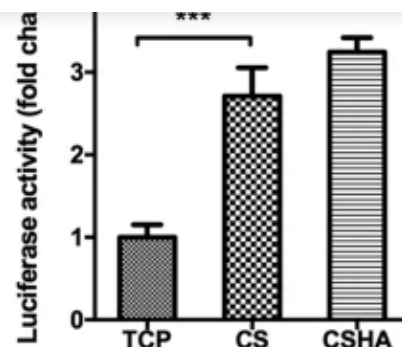
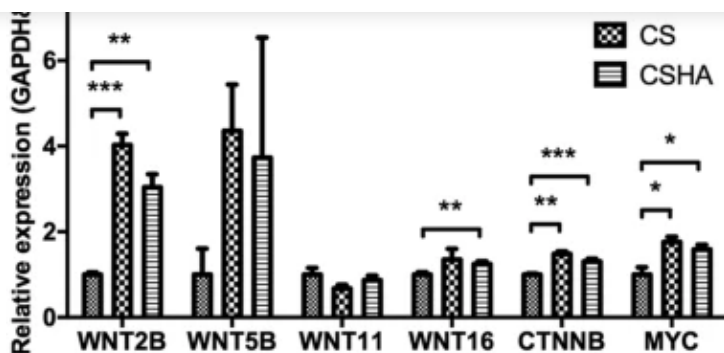
Figure 5: Characterization of quiescent population for HT29 and Huh7.



(a) Ki-67 and PI negative population representing the quiescent population. (b) p16 and p21 mRNA expressions after 72 hrs of culture. (c) The protein expression levels of p16 and p21 after 72 hrs of culture. Each bar represents the means of three determinations \pm SD. * $p < 0.05$, ** $p < 0.01$, *** $p < 0.001$ among the indicated groups.

on CS and CSHA membranes ([Fig. 6a](#)). Wnt signaling downstream genes, CTNNB and MYC, were also upregulated in HT29 on CS and CSHA membranes ([Fig. 6a](#)). The Wnt/ β -catenin reporter assay (TOP-flash) showed that CS substrates activated Wnt/ β -catenin signaling in HT29 but not in Huh7 ([Fig. 6b](#), [Supplementary Fig. S6](#)). The expression of noncanonical Wnt ligands, WNT5B, WNT11, and WNT16, were upregulated in Huh7 cells on CS and CSHA membranes ([Fig. 6c](#)). Since Wnt5-Frizzled2 could activate STAT3 phosphorylation in cancer cells and increase CSC properties, we further checked the activation of STAT3. In [Fig. 6d](#), the phosphorylated STAT3 was increased in Huh7 by culturing on CS and CSHA membranes. Meanwhile, we did not observe any change of STAT3 phosphorylation in HT29 ([Supplementary Fig. S6](#)). To confirm the role of Wnt signaling, we used IWP-4 to inhibit Wnt signaling in both HT29 and Huh7 cells ([Supplementary Fig. S7](#)). The expression levels of stemness genes as OCT4, NANOG, and CD133 decreased in the cancer cells on both CS and CSHA membranes with IWP-4 treatment. In addition, the migration ability promoted by CS and CSHA membranes was reduced with IWP-4 treatment. The cell morphology was not significantly changed between treated cells and non-treated cells ([Supplementary Fig. S7](#)).

Figure 6: Activation of canonical and noncanonical Wnt signaling pathways for cancer cells on CS and CSHA membranes.

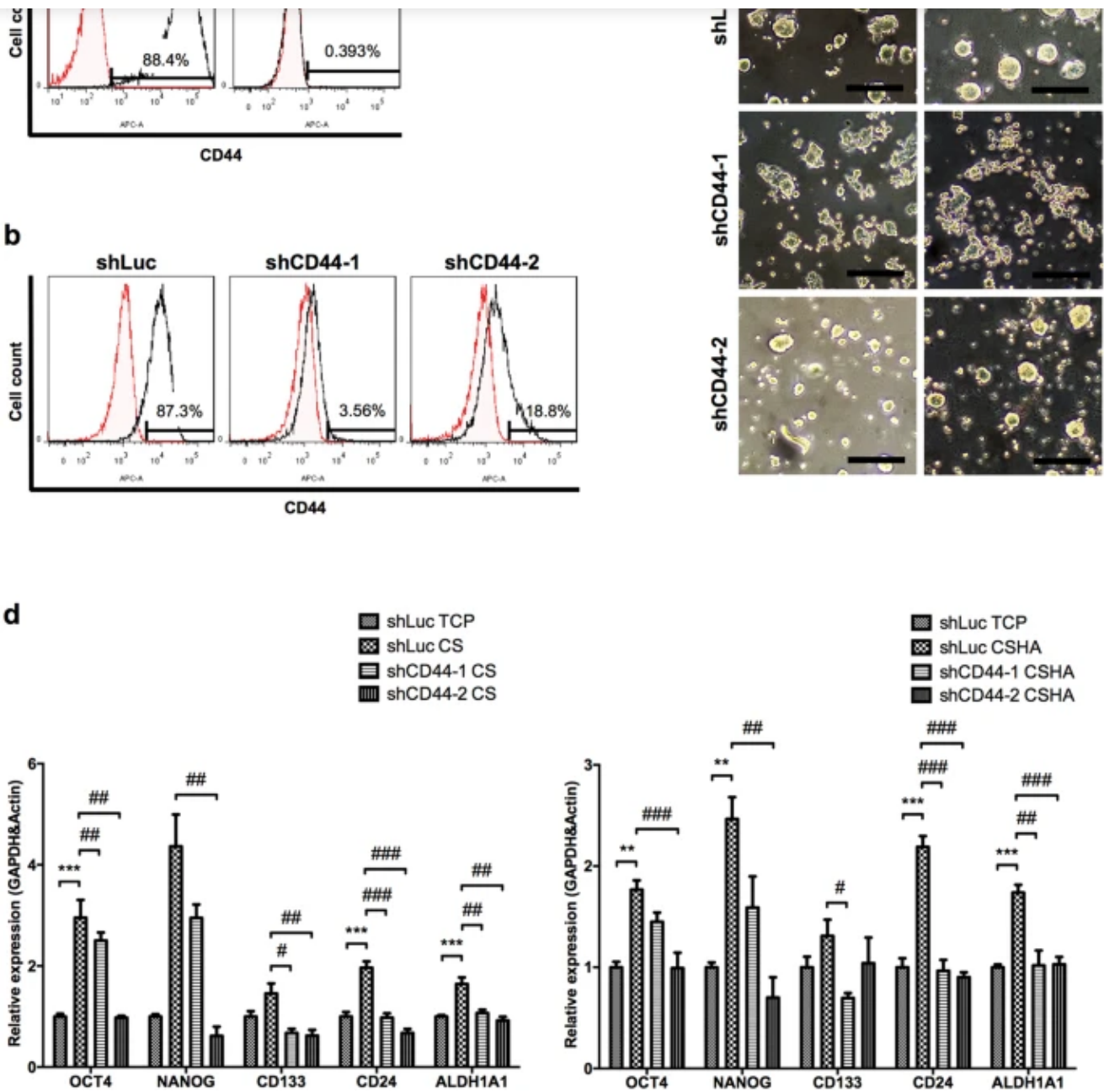


(a) The mRNA expression levels of WNT2B, WNT5B, WNT11, WNT16, CTNNB, and MYC in HT29 after 72 hrs of culture. (b) TOP-flash luciferase reporter assay showed the activation of canonical Wnt signaling in HT29 grown on CS and CSHA membranes. (c) The mRNA expression levels of WNT2B, WNT5B, WNT11, WNT16, CTNNB, and MYC in Huh7 after 72 hrs of culture. (d) Phosphorylation of STAT3 by western blot for Huh7 on CS and CSHA membranes after 72 hrs of culture. The lower bar chart indicated the quantification of protein band. Each bar represents the means of three determinations \pm SD. * $p < 0.05$, ** $p < 0.01$, *** $p < 0.001$ among the indicated group.

The CD44-dependent effect of the colon cancer cells cultured on CS and CSHA membranes

target of Wnt signaling, in the cancer cells grown on CS and CSHA membranes, knockdown of CD44 expression in HT29 was performed ([Fig. 7b](#)). The experimental results demonstrated that knockdown of CD44 significantly deprived HT29 of spheroid formation ([Fig. 7c](#)) and decreased the expression of stemness genes OCT4 and NANOG, CSC marker genes CD133 and CD24, as well as ALDH1A1 gene for HT29 both on CS and CSHA membranes ([Fig. 7d](#)).

Figure 7: The effect of knockdown of CD44 receptor on morphology and gene expressions.



(a) CD44 expressions in wild type (WT) HT29 and Huh7 by flow cytometry. (b) CD44 expressions in lentivirus-treated HT29 (shLuc, shCD44-1, and shCD44-2). (c) The morphology of lentivirus-treated HT29 after 72 hrs of culture. Scale bar represents 200 μ m. (d) The mRNA expression levels of OCT4, NANOG, CD133, CD24, and ALDH1A1 for lentivirus-treated HT29 after 72 hrs of culture. Each bar represents the means of three determinations \pm SD. ** $p < 0.01$, *** $p < 0.001$ with respect to the shLuc TCP group. $p < 0.05$, $p < 0.01$, $p < 0.001$ with respect to the shLuc CS and shLuc CSHA group. #####

tumor formation and development¹³. In order to mimic *in vivo* tumor microenvironments, 3D culture with biomaterials is developed to investigate tumor biology¹⁴. However, scaffold matrix-embedded 3D cell culture is complicated and has difficulty in harvesting the cancer cells for further studies. Here, we used chitosan substrates to create a simple and convenient system to culture cancer cells. We showed that chitosan alone could increase cancer cell stemness properties and tumor progression.

We observed that chitosan and HA-grafted chitosan could induce diverse morphology of various cancer cell types. Cellular phenotypes, CD44 expression and cellular properties of cell lines might affect the aggregation ability on CS and CSHA. We found cells with epithelial-like phenotype and/or higher CD44 expression tended to form colonies or spheroids on CS and CSHA, in contrast to cells with mesenchymal-like phenotype and/or CD44-negative. On the other hand, CSHA provided an environment for cells to aggregate more easily than CS. Based on the cell morphology on TCP plates, HT29 and SW480 have epithelial-like phenotype, and DLD-1 and HCT116 have mesenchymal-like phenotype. As shown in our [Fig. 1](#) and [Supplementary Fig. S1](#), only HT29 could form spheroids on CS membranes but DLD-1 and HCT116 could not. SW480 was an exception. Previous studies^{32,33} and we (data not shown) revealed that SW480 could not form spheroids in the sphere forming assay. It also failed to aggregate on both CS and CSHA. HT29, DLD-1 and HCT116 are all CD44-positive cells and able to aggregate on CSHA membranes. We also observed the similar phenomenon among HCC cell lines.

Previous studies demonstrated ATP-binding cassette (ABC) transporters and aldehyde dehydrogenase (ALDH) enzymes contributed to drug resistance of cancer cells^{34,35}. In the current study, chitosan not only elevated the cell viability of HT29 and Huh7 under 5-Fu and doxorubicin treatment but also upregulated the expression levels of ABCG2 and ALDH. Interestingly, our results showed Huh7 had higher ALDH enzyme activity while the gene expression of ALDH1A1 in Huh7 was not significantly changed on CS

colon cancer and HCC cells—and activates some pathways associated with migration such as Cdc42 and Ras⁴⁰. MMP14, a membrane-type matrix metalloproteinase (MMP), promotes cancer invasion and metastasis⁴¹. Our results revealed that chitosan increased the migration ability and expression levels of CXCR4 and MMP14 in both HT29 and Huh7. Knockdown of MMP14 could reduce the effect of chitosan substrates on cell motility in both cell lines. However, knockdown of CXCR4 by several shRNA sequences in Huh7 could not significantly decrease the migration ability in CS and CSHA groups. We assumed that dozens of genes and cellular properties might be changed while cells grew on CS or CSHA. Several motility-related genes might be upregulated to enhance the cellular migration ability by CS and CSHA. Therefore, although CXCR4 plays an important role in the migration of Huh7 cells⁴², knockdown of CXCR4 gene might not significantly affect the migration of Huh7 cells in CS and CSHA groups. According to GSEA analysis, we also found genes related to Cdc42 and Ras pathways were upregulated on chitosan membranes. In addition, mTOR, a downstream effector of the PI3K/AKT pathway has been reported to affect tumor progression⁴³. By means of the GSEA analysis, we found that the mTOR pathway associated genes were upregulated for HT29 cells on chitosan membranes. GSEA data also revealed that the upregulated genes were associated with the EGFR or Myc target gene set. Several studies have shown that EGFR and Myc are often overexpressed in human carcinomas and play crucial roles in tumorigenesis^{44,45}. On the other hand, we observed both CS and CSHA had similar stemness-induced effects with varying degrees on the cancer cells. CSHA was a biomaterial with grafted HA on the surface of CS. Therefore, HA was the major component of CSHA to interact with the cancer cells. Even though previous study suggested the structure of HA is partially similar to chitosan³⁰, CS and CSHA might create similar but different microenvironments to affect the cancer cells. Taken together, chitosan alone may enhance the cancer cell migration ability and drug resistance and may activate several tumorigenesis-associated pathways.

Recent literature showed that CSCs, distinct subpopulation cells in the tumor, contributed to cancer heterogeneity that increased the complexity within a tumor and

microenvironments¹⁴. Our results showed that the chitosan culture system could mimic tumor microenvironments and elevate the expression levels of stemness and CSC marker genes. The heatmap analysis of microarray data demonstrated that the upregulated genes of HT29 cultured on chitosan substrates were correlated with the stemness gene set of normal Lgr5-positive intestinal stem cells⁴⁶. CSC marker genes of HT29 cells were also upregulated on chitosan membranes. These data revealed that chitosan might increase stemness-related genes. We further verified these data by RT-PCR analyses and CSC-associated functional assays. We found that the core stemness transcription factors, OCT4 and NANOG, increased significantly for both HT29 and Huh7. Besides, the expression levels of CSC markers, CD133, CD24, CD44, CD90, and EpCAM were enhanced. These CSC markers are also required for maintenance of stemness properties of CSCs through several signaling pathways^{47,48}. The factors associated with drug resistance, ABCG2, and ALDH, were also regarded as the CSC markers^{49,50}. Moreover, CSCs maintain CSC pools through their self-renewal ability that could be evaluated by sphere forming assay⁵¹. The results of ELDA sphere forming assay revealed that the cancer cells on the chitosan membranes increased not only self-renewal ability but also the CSC frequency. Chitosan also increased the BMI1 expression, the crucial regulator of self-renewal⁵². Additionally, some CSCs in the tumors stay at quiescent states, regarded as G₀ phase in cell cycles, to prevent CSC exhaustions caused by differentiation⁵³. At quiescent states, CSCs could resist anti-proliferation drugs and then escape from cytotoxic chemotherapies⁵⁴. Our results revealed that chitosan increased quiescent population and the expression of quiescence regulators p16 and p21 in both HT29 and Huh7. These results suggested chitosan might increase CSC population via increasing quiescence of CSCs. Taken together, we demonstrated that chitosan substrates promoted the characteristics of CSCs such as migration ability, drug resistance, self-renewal capacity, and quiescent population.

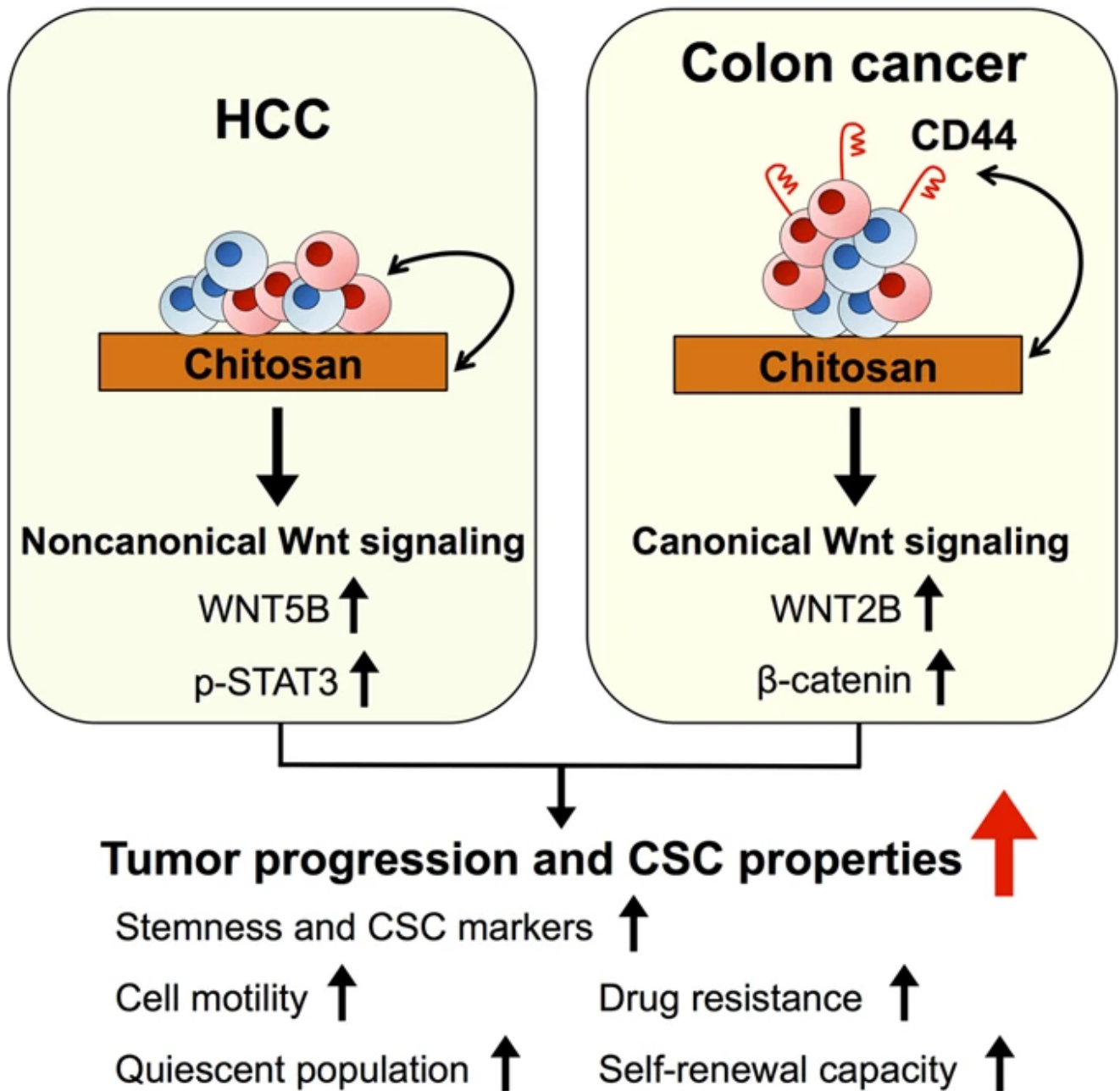
A few biomaterials were used in cancer cell culture systems to imitate the tumor microenvironments¹⁴. These biomaterial scaffolds facilitated cancer cells to form 3D multicellular spheroids that mimic the solid tumor *in vivo*. Other reports showed that

regardless if cells were assembled into 3D cellular spheroids. Chitosan itself may provide external signals from microenvironments to alter the fate of cancer cells, but the interactions between chitosan and cancer cells were relatively unexplored. Multiple signaling pathways including Wnt/ β -catenin, Notch, and Hedgehog regulate the CSC properties⁸. Colon CSC population possesses high Wnt activity⁹. Hyperactivation of Wnt/ β -catenin signaling could even trigger differentiated epithelial cells to convert into tumor-initiating cells⁵⁷. Noncanonical Wnt signaling also enhances CSC characteristics in HCC and colon cancers¹⁰. Noncanonical Wnt ligand can increase EMT in HCC cells through STAT3 activation. Here, we showed that chitosan significantly increased the phosphorylation of STAT3 in Huh7 HCC cells but not in HT29 colon cancer cells. Nevertheless, we observed chitosan increased the Wnt/ β -catenin reporter activity in HT29 cells. Thus, we suggested that the chitosan culture system increased canonical and noncanonical Wnt signalings in HT29 and Huh7 cancer cells, respectively. On the other hand, Rao *et al.* recently revealed that chitosan nanoparticles could bind to cell membranes of CSCs via CD44³⁰. The chemical structure of chitosan partially resembles HA, a major ligand of CD44 receptors. Thus, they assumed that chitosan may specifically target CD44^{positive} CSCs. Additionally, CD44 isoforms on CSCs could couple with other signaling pathways, such as c-Met, which could promote their stemness properties⁵⁸. CD44 is a Wnt/ β -catenin target gene and can also activate Wnt/ β -catenin in a concentration-dependent manner via modulating Wnt-LRP6 receptor complex⁵⁹. Our results demonstrated that knockdown of the CD44 expression in HT29 would abolish their ability to form multicellular spheroids on chitosan membranes and downregulate the stemness and CSC marker genes. Taken together, chitosan substrates increase CSC properties of HT29 colon cancer cells and Huh7 HCC cells and probably are associated with different Wnt signaling pathways.

Chitosan modified with other molecules has been recently used as culture systems for the investigation of tumor progressions and has been shown to increase the cancer stemness^{23,24,25,26}. In the current study, we considered that the pristine chitosan per se could promote the properties of CSCs including migration ability, drug resistance,

pathways in CD44⁺ colon cancer and CD44⁺ HCC, respectively (Fig. 8). This simple culture system mimics *in vivo* microenvironments of CSCs and creates a novel platform for CSC research and cancer drug development.

Figure 8



Chitosan might promote tumor progression and CSC properties in association with canonical or noncanonical Wnt signalings in different cancer cells.

The molecular weight of the chitosan powder (Sigma) was 510 kDa and the degree of deacetylation was 77%. The molecular weight of HA (SciVision Biotech) was about 2500 kDa. CS and CSHA membranes were prepared as previously reported²⁹. Briefly, chitosan was dissolved in 1% acetic acid solution and coated on each well of 6-well plate. CS membranes were formed after evaporation of solvent in a laminar flow cabinet for 24 hrs. CS membranes were soaked in 0.5 N sodium hydroxide for 30 minutes, and washed with phosphate buffered saline (PBS) three times. For the preparation of CSHA membranes, HA solution was added in each chitosan-coated well with the amount of 0.5 mg per cm² of CS membranes. CSHA membranes were crosslinked with ethyl (dimethylaminopropyl) carbodiimide/N-hydroxysuccinimide (EDC/NHS) solution with a weight ratio of HA/EDC/NHS adjusted to 1:1.84:0.23 at pH 5.5. Then, CSHA membranes were washed with PBS three times to remove unbound HA.

Cell culture and cell seeding on CS and CSHA membranes

The human colon cancer cell lines HT29 (ATCC) and DLD-1 (ATCC) were cultured with Roswell Park Memorial Institute (RPMI, Life Technologies) 1640 medium. The human colon cancer cell lines, HCT116 (ATCC) and SW480 (ATCC), and HCC cell lines Huh7 (JCRB), HepG2 (ATCC), Hep3B (ATCC), and SKHep-1 (ATCC) were cultured with Dulbecco's modified Eagle's medium (DMEM, Life Technologies). Both RPMI and DMEM medium contained 10% fetal bovine serum (FBS, GeneDireX) and 1% penicillin, streptomycin, and glutamine (PSG, Life Technologies). Cells were maintained at 37 °C in a humidified atmosphere of 5% CO₂ within 10 passages. Cells were seeded on CS and CSHA membranes or tissue culture polystyrene (TCP) plates as the control group. The microscopy and real-time Cultured Cell Monitoring System were used for the observation of cell morphology. For Wnt signaling inhibition experiment, cells were treated with IWP-4 (20 μM, STEMCELL Technologies) for 24 hrs after seeded on CS and CSHA membranes.

Transwell migration assay

10⁵ cells/well) were harvested and plated into the upper compartment which contained 300 μ L serum-free medium, while the lower compartment contained 500 μ L medium with 10% FBS. Following 18 hrs of incubation at 37 °C in 5% CO₂, non-migrated cells were removed from the upper surface of the transwell, and the migrated cells remaining on the lower surface were fixed with methanol for 10 min and counted after staining with crystal violet for 1 hr.

Drug resistance assay

While seeding on CS and CSHA membranes or TCP plates, HT29 and Huh7 were treated with varying concentrations of 5-Fluorouracil (Sigma) and doxorubicin (Sigma) for 72 hrs, respectively. Cell viability was evaluated using MTT (Sigma) assay according to the manufacturer's instructions.

Flow cytometry analysis

HT29 and Huh7 were stained with FITC-conjugated CD133 (Miltenyi Biotec) and PE-conjugated CD13 (BD Bioscience) at 4 °C for 1 hr, respectively. Cell staining with FITC-conjugated IgG (Biolegend) or PE-conjugated IgG (Biolegend) was used as the isotype control group. Aldehyde dehydrogenase (ALDH) activity was measured using ALDEFLUOR reagent (STEMCELL Technologies) with or without DEAB (ALDH inhibitor) following the manufacturer's instructions. For analysis of side population, cells were incubated in 10% FBS medium containing 5 μ g/mL Hoechst 33342 (Life Technologies) at 37 °C for 90 minutes. In control groups, cells were incubated with Hoechst 33342 in the presence of 50 μ M Verapamil (Sigma). For quiescence assay, the quiescence (G₀ phase) was defined as the population of Ki-67 negative cells in G₀/G₁ phase divided with propidium iodide (PI). In the assay, Foxp3/Transcription Factor Staining Buffer Set (eBioscience) was used for fixation and permeabilization following the manufacturer's instructions. Cells were incubated with anti-human Ki-67 biotin (eBioscience) at room temperature for 1 hr. Then, cells were incubated with APC-conjugated streptavidin (Biolegend), 1 mg/mL RNase A (Sigma) and 30 μ g/mL PI (Life Technologies) at room temperature for 30 minutes. After the incubation, all samples were resuspended,

Microarray data analysis

Total RNA was prepared using TriPure Isolation Reagent (Roche Life Science). cRNA was amplified and labelled using a Quick Amp Labelling Kit (Agilent Technologies) and hybridized to a 8 × 60 k v2 array chips (Agilent Technologies) according to the manufacturer's instructions. The hybridized microarray slides were scanned using an Agilent scanner. The relative hybridization intensities and background hybridization values were calculated using Feature Extraction Software version 9.5.1.1 (Agilent Technologies). The raw signal intensities and flags for each probe were calculated from the hybridization intensities and spot information according to the procedures recommended by Agilent Technologies. Briefly, a signal intensity less than 1 was corrected to 1 (not detected), and then the 75th percent shift normalization was conducted. Unless otherwise specified, data processing and analysis were performed using the statistical software R. Gene Set Enrichment Analysis (GSEA)⁶⁰ was performed according to the standard procedure. Stemness gene set was adopted from the publication by Munoz, J *et al.*⁴⁶.

Sphere forming assay and 3D culture system

ELDA (extreme limiting dilution analysis) was performed to evaluate self-renewal capacity⁶¹. Briefly, cells were dissociated into single cell suspensions and plated at the concentration of 100, 50 and 25 cells per well, in Ultra-Low attachment 96-well plate (Corning) with serum-free sphere medium containing 2% B27 supplement (Gibco), 20 ng/mL epidermal growth factor (EGF) (PeproTech), and 10 ng/mL basic fibroblast growth factor (bFGF) (PeproTech). After 10 days of culture, spheres were stained by Hoechst 33342 (Life Technologies) and counted by IN Cell Analyzer 2000 (GE Healthcare Life Sciences). The frequency of sphere-forming cells was determined using the ELDA web-based tool at <http://bioinf.wehi.edu.au/software/elda>. Non-adherent and long-term culture was used for 3D sphere culture system. Briefly, cells were seeded into the agarose-coated plate with serum-free sphere medium containing 2% B27 supplement (Gibco), 20 ng/mL EGF (PeproTech), 10 ng/mL bFGF (PeproTech). After 9 days culture, spheres were harvested and analyzed by RT-PCR.

trans luciferase reporter construct contains 3 copies of the TCT/LEF-binding site (AAGATCAAAGGGGGT) upstream of a TK minimal promoter. Cells were transfected with TOP-flash and pmCherry-C1 (Clontech) plasmid by JetPRIME reagent (Polyplus-transfection) following the manufacturer's protocol. After 24 hrs of incubation, cells were harvested and seeded on TCP plates, CS and CSHA membranes for 48 hrs of culture. For luminescence measurement, cell lysates were transferred to white 96-well microplate and then the measurement was performed using Orion L Microplate Luminometer (Berthold Detection Systems). Fluorescence intensity of mCherry was measured by FlexStation 3 microplate reader (Molecular Devices) for internal control.[®]

Western blot

Cells were lysed in cold radioimmunoprecipitation assay (RIPA) lysis buffer containing protease inhibitor (Sigma) and phosphatase inhibitor (Sigma) and subjected to sodium dodecyl sulfate polyacrylamide gel electrophoresis (SDS-PAGE). Proteins were transferred onto polyvinylidene difluoride (PVDF) membranes and probed with primary antibodies. The protein expression levels were normalized with GAPDH (Millipore). The information of the antibodies was shown in [Supplementary Table S2](#).[®]

Lentivirus knockdown system

The plasmids of short hairpin RNA (shRNA) targeting CD44, MMP14, and CXCR4 were purchased from Academia Sinica, Taipei, Taiwan. To prepare shRNA lentiviral stocks, HEK293T cells were transfected with three lentivirus-packaging plasmids (pMDLg/pRPE, pMD2G, pRSV-Rev, Addgene) and CD44 shRNA (shCD44-1 or shCD44-2), MMP14 shRNA (shMMP14-1 or shMMP14-2), CXCR4 shRNA (shCXCR4-1 or shCXCR4-2), or luciferase shRNA (shLuc) plasmids by JetPRIME (Polyplus-transfection) reagent following the manufacturer's protocol. After 48 hrs of incubation, supernatants containing shRNA lentivirus were collected by centrifugation with 8.5% polyethylene glycol 6000 and 0.3 M sodium chloride. Then, lentivirus was introduced into HT29 or Huh7 for 24 hrs, followed by selection with puromycin (1 µg/mL) for 48 hrs. Flow cytometry and western blot were used to confirm the knockdown efficiency.

prepared using the High-Capacity cDNA Reverse Transcription Kit (Applied Biosystem). RT-PCR was performed using iQ SYBR green detection system in CFX96 (Bio-Rad). The expression level of target genes was normalized to GAPDH and β -actin. The primers used for RT-PCR were shown in [Supplementary Table S1](#).

Statistical analysis

Data were expressed as means \pm SD. Statistical significance of results was evaluated using ANOVA and further analyzed by Tukey's multiple comparison test. All statistical tests were performed using GraphPad Prism v.5.0. P-value were displayed on the graphs using a single asterisk for values between 0.05 to 0.01, two asterisk for values between 0.01 to 0.001, and three asterisks for values below 0.001.

Additional Information

How to cite this article: Chang, P.-H. *et al.* Chitosan promotes cancer progression and stem cell properties in association with Wnt signaling in colon and hepatocellular carcinoma cells. *Sci. Rep.* **7**, 45751; doi: 10.1038/srep45751 (2017).

Publisher's note: Springer Nature remains neutral with regard to jurisdictional claims in published maps and institutional affiliations.

References

- 1 Siegel, R. L., Miller, K. D. & Jemal, A. Cancer statistics, 2016. *CA Cancer J Clin.* **66**, 7–30 (2016).
 - 2 Ishizawa, K. et al. Tumor-initiating cells are rare in many human tumors. *Cell Stem Cell.* **7**, 279–282 (2010).
-

- 4 Li, F., Tiede, B., Massague, J. & Kang, Y. Beyond tumorigenesis: cancer stem cells in metastasis. *Cell Res.* **17**, 3–14 (2007).
- 5 Zeuner, A. et al. Elimination of quiescent/slow-proliferating cancer stem cells by Bcl-XL inhibition in non-small cell lung cancer. *Cell Death Differ.* **21**, 1877–1888 (2014).
- 6 Medema, J. P. Cancer stem cells: the challenges ahead. *Nat Cell Biol.* **15**, 338–344 (2013).
- 7 Wicha, M. S. Targeting self-renewal, an Achilles' heel of cancer stem cells. *Nat Med.* **20**, 14–15 (2014).
- 8 Takebe, N. et al. Targeting Notch, Hedgehog, and Wnt pathways in cancer stem cells: clinical update. *Nat Rev Clin Oncol.* **12**, 445–464 (2015).
- 9 Vermeulen, L. et al. Wnt activity defines colon cancer stem cells and is regulated by the microenvironment. *Nat Cell Biol.* **12**, 468–476 (2010).
- 10 Gujral, T. S. et al. A noncanonical Frizzled2 pathway regulates epithelial-mesenchymal transition and metastasis. *Cell.* **159**, 844–856 (2014).
- 11 Marotta, L. L. et al. The JAK2/STAT3 signaling pathway is required for growth of CD44(+)CD24(-) stem cell-like breast cancer cells in human tumors. *J Clin Invest.* **121**, 2723–2735 (2011).
- 12 Vidal, S. J., Rodriguez-Bravo, V., Galsky, M., Cordon-Cardo, C. & Domingo-

- 13 Hanahan, D. & Coussens, L. M. Accessories to the crime: functions of cells recruited to the tumor microenvironment. *Cancer Cell*. **21**, 309–322 (2012).
- 14 Gu, L. & Mooney, D. J. Biomaterials and emerging anticancer therapeutics: engineering the microenvironment. *Nat Rev Cancer*. **16**, 56–66 (2016).
- 15 Fischbach, C. et al. Cancer cell angiogenic capability is regulated by 3D culture and integrin engagement. *Proc Natl Acad Sci USA* **106**, 399–404 (2009).
- 16 Yamada, K. M. & Cukierman, E. Modeling tissue morphogenesis and cancer in 3D. *Cell*. **130**, 601–610 (2007).
- 17 Kaemmerer, E. et al. Gelatine methacrylamide-based hydrogels: an alternative three-dimensional cancer cell culture system. *Acta Biomater*. **10**, 2551–2562 (2014).
- 18 Fong, E. L. et al. Modeling Ewing sarcoma tumors *in vitro* with 3D scaffolds. *Proc Natl Acad Sci USA*. **110**, 6500–6505 (2013).
- 19 Borovski, T., De Sousa, E. M. F., Vermeulen, L. & Medema, J. P. Cancer stem cell niche: the place to be. *Cancer Res*. **71**, 634–639 (2011).
- 20 Plaks, V., Kong, N. & Werb, Z. The cancer stem cell niche: how essential is the niche in regulating stemness of tumor cells? *Cell Stem Cell*. **16**, 225–238 (2015).
- 21 Chang, C. et al. A laminin 511 matrix is regulated by TAZ and functions as the ligand for the alpha6Bbeta1 integrin to sustain breast cancer stem cells. *Genes*

- 22 Cheung, R. C., Ng, T. B., Wong, J. H. & Chan, W. Y. Chitosan: An Update on Potential Biomedical and Pharmaceutical Applications. *Mar Drugs*. **13**, 5156–5186 (2015).

- 23 Shanmugasundaram, N. et al. Collagen-chitosan polymeric scaffolds for the *in vitro* culture of human epidermoid carcinoma cells. *Biomaterials*. **22**, 1943–1951 (2001).

- 24 Florczyk, S. J. et al. 3D porous chitosan-alginate scaffolds: a new matrix for studying prostate cancer cell-lymphocyte interactions *in vitro* . *Adv Healthc Mater*. **1**, 590–599 (2012).

- 25 Kievit, F. M. et al. Proliferation and enrichment of CD133(+) glioblastoma cancer stem cells on 3D chitosan-alginate scaffolds. *Biomaterials*. **35**, 9137–9143 (2014).

- 26 Sims-Mourtada, J., Niamat, R. A., Samuel, S., Eskridge, C. & Kmiec, E. B. Enrichment of breast cancer stem-like cells by growth on electrospun polycaprolactone-chitosan nanofiber scaffolds. *Int J Nanomedicine*. **9**, 995–1003 (2014).

- 27 Huang, G. S., Dai, L. G., Yen, B. L. & Hsu, S. H. Spheroid formation of mesenchymal stem cells on chitosan and chitosan-hyaluronan membranes. *Biomaterials*. **32**, 6929–6945 (2011).

- 28 Zoller, M. CD44: can a cancer-initiating cell profit from an abundantly expressed molecule? *Nat Rev Cancer*. **11**, 254–267 (2011).

- 29 Huang, Y. J. & Hsu, S. H. Acquisition of epithelial-mesenchymal transition and cancer stem-like phenotypes within chitosan-hyaluronan membrane-derived 3D

- 30 Rao, W. et al. Chitosan-Decorated Doxorubicin-Encapsulated Nanoparticle Targets and Eliminates Tumor Reinitiating Cancer Stem-like Cells. *ACS Nano*. **9**, 5725–5740 (2015).

- 31 Wielenga, V. J. et al. Expression of CD44 in Apc and Tcf mutant mice implies regulation by the WNT pathway. *Am J Pathol*. **154**, 515–523 (1999).

- 32 Leng, Z. et al. Krüppel-Like Factor 4 Acts as an Oncogene in Colon Cancer Stem Cell-Enriched Spheroid Cells. *PLoS One*. **8** (2013).

- 33 Oshima, N. et al. Induction of cancer stem cell properties in colon cancer cells by defined factors. *PLoS One*. **9**, e101735 (2014).

- 34 Fletcher, J. I., Haber, M., Henderson, M. J. & Norris, M. D. ABC transporters in cancer: more than just drug efflux pumps. *Nat Rev Cancer*. **10**, 147–156 (2010).

- 35 Tanei, T. et al. Association of breast cancer stem cells identified by aldehyde dehydrogenase 1 expression with resistance to sequential Paclitaxel and epirubicin-based chemotherapy for breast cancers. *Clin Cancer Res*. **15**, 4234–4241 (2009).

- 36 Ma, S. et al. Aldehyde dehydrogenase discriminates the CD133 liver cancer stem cell populations. *Mol Cancer Res*. **6**, 1146–1153 (2008).

- 37 Marcato, P., Dean, C. A., Giacomantonio, C. A. & Lee, P. W. K. Aldehyde dehydrogenase: Its role as a cancer stem cell marker comes down to the specific isoform. *Cell Cycle*. **10**, 1378–1384 (2011).

-
- 39 Liu, H. et al. Roles of chemokine receptor 4 (CXCR4) and chemokine ligand 12 (CXCL12) in metastasis of hepatocellular carcinoma cells. *Cell Mol Immunol.* **5**, 373–378 (2008).
-
- 40 Wong, D. & Korz, W. Translating an Antagonist of Chemokine Receptor CXCR4: from bench to bedside. *Clin Cancer Res.* **14**, 7975–7980 (2008).
-
- 41 Zarrabi, K. et al. Inhibition of matrix metalloproteinase 14 (MMP-14)-mediated cancer cell migration. *J Biol Chem.* **286**, 33167–33177 (2011).
-
- 42 Liu, H., Liu, Y., Liu, W., Zhang, W. & Xu, J. EZH2-mediated loss of miR-622 determines CXCR4 activation in hepatocellular carcinoma. *Nature Communications.* **6**, 8494 (2015).
-
- 43 Populo, H., Lopes, J. M. & Soares, P. The mTOR signalling pathway in human cancer. *Int J Mol Sci.* **13**, 1886–1918 (2012).
-
- 44 Normanno, N. et al. Epidermal growth factor receptor (EGFR) signaling in cancer. *Gene.* **366**, 2–16 (2006).
-
- 45 Dang, C. V. MYC on the path to cancer. *Cell.* **149**, 22–35 (2012).
-
- 46 Munoz, J. et al. The Lgr5 intestinal stem cell signature: robust expression of proposed quiescent '+4' cell markers. *EMBO J.* **31**, 3079–3091 (2012).
-
- 47 Munz, M., Baeuerle, P. A. & Gires, O. The emerging role of EpCAM in cancer and

- 48 Pietras, A. et al. Osteopontin-CD44 signaling in the glioma perivascular niche enhances cancer stem cell phenotypes and promotes aggressive tumor growth. *Cell Stem Cell*. **14**, 357–369 (2014).
-
- 49 Ginestier, C. et al. ALDH1 is a marker of normal and malignant human mammary stem cells and a predictor of poor clinical outcome. *Cell Stem Cell*. **1**, 555–567 (2007).
-
- 50 Bleau, A. M. et al. PTEN/PI3K/Akt pathway regulates the side population phenotype and ABCG2 activity in glioma tumor stem-like cells. *Cell Stem Cell*. **4**, 226–235 (2009).
-
- 51 Wang, Y. J., Bailey, J. M., Rovira, M. & Leach, S. D. Sphere-forming assays for assessment of benign and malignant pancreatic stem cells. *Methods Mol Biol*. **980**, 281–290 (2013).
-
- 52 Liu, S. et al. Hedgehog signaling and Bmi-1 regulate self-renewal of normal and malignant human mammary stem cells. *Cancer Res*. **66**, 6063–6071 (2006).
-
- 53 Moore, N. & Lyle, S. Quiescent, slow-cycling stem cell populations in cancer: a review of the evidence and discussion of significance. *J Oncol*. **2011** (2011).
-
- 54 Essers, M. A. & Trumpp, A. Targeting leukemic stem cells by breaking their dormancy. *Mol Oncol*. **4**, 443–450 (2010).
-
- 55 Kolenda, J. et al. Effects of hypoxia on expression of a panel of stem cell and chemoresistance markers in glioblastoma-derived spheroids. *J Neurooncol*. **103**, 43–58 (2011).

12, 39 (2014).

-
- 57 Schwitalla, S. et al. Intestinal tumorigenesis initiated by dedifferentiation and acquisition of stem-cell-like properties. *Cell*. **152**, 25–38 (2013).
-
- 58 Todaro, M. et al. CD44v6 is a marker of constitutive and reprogrammed cancer stem cells driving colon cancer metastasis. *Cell Stem Cell*. **14**, 342–356 (2014).
-
- 59 Schmitt, M., Metzger, M., Gradl, D., Davidson, G. & Orian-Rousseau, V. CD44 functions in Wnt signaling by regulating LRP6 localization and activation. *Cell Death Differ*. **22**, 677–689 (2015).
-
- 60 Subramanian, A. et al. Gene set enrichment analysis: a knowledge-based approach for interpreting genome-wide expression profiles. *Proc Natl Acad Sci USA* **102**, 15545–15550 (2005).
-
- 61 Hu, Y. & Smyth, G. K. ELDA: extreme limiting dilution analysis for comparing depleted and enriched populations in stem cell and other assays. *J Immunol Methods*. **347**, 70–78 (2009).
-
- 62 Molenaar, M. et al. XTcf-3 transcription factor mediates beta-catenin-induced axis formation in *Xenopus* embryos. *Cell*. **86**, 391–399 (1996).
-

Acknowledgements

We appreciated Dr. Shu-Chen Wei (Department of Internal Medicine, National Taiwan University Hospital and College of Medicine, Taipei, Taiwan) gave us MMP14 antibody.

PDF herunterladen

the excellent technical assistance of Technology Commons, College of Life Science,
National Taiwan University (Taiwan).

Author information

Authors and Affiliations

Department of Biochemical Science and Technology, niChe Lab for Stem Cell and Regenerative Medicine, National Taiwan University, Taipei, 10617, Taiwan
Po-Hsiang Chang, Hsiao-Mei Chao & Edward Chern

Department of Regenerative Medicine, Yokohama City University Graduate School of Medicine, Kanagawa, 236-0004, Japan
Keisuke Sekine

Department of Pathology, Wan Fang Hospital, Taipei Medical University, Taipei, 11696, Taiwan
Hsiao-Mei Chao

Institute of Polymer Science and Engineering, National Taiwan University, Taipei, 10617, Taiwan
Shan-hui Hsu

Contributions

P.C., H.C., S.H. and E.C. conceived and designed the experiments. P.C., K.S. and E.C. performed the experiments and analyzed the data. P.C., K.S., S.H., H.C. and E.C. contributed reagents/materials/analysis tools. P.C., H.C., S.H. and E.C. wrote the manuscript.

Corresponding authors

Correspondence to [Shan-hui Hsu](#) or [Edward Chern](#).

Ethics declarations

Competing interests

The authors declare no competing financial interests.

Supplementary information

[Supplementary Video 2 \(MOV 990 kb\)](#)

Rights and permissions

This work is licensed under a Creative Commons Attribution 4.0 International License. The images or other third party material in this article are included in the article's Creative Commons license, unless indicated otherwise in the credit line; if the material is not included under the Creative Commons license, users will need to obtain permission from the license holder to reproduce the material. To view a copy of this license, visit <http://creativecommons.org/licenses/by/4.0/>

[Reprints and Permissions](#)

About this article

Cite this article

Chang, PH., Sekine, K., Chao, HM. *et al.* Chitosan promotes cancer progression and stem cell properties in association with Wnt signaling in colon and hepatocellular carcinoma cells. *Sci Rep* **7**, 45751 (2017). <https://doi.org/10.1038/srep45751>

Received

05 October 2016

Accepted

06 March 2017

Published

03 April 2017

DOI

<https://doi.org/10.1038/srep45751>

Share this article

Anyone you share the following link with will be able to read this content:

[Get shareable link](#)

This article is cited by

Targeting cancer stem cells with polymer nanoparticles for gastrointestinal cancer treatment

Yao Sun, Bo Li ... Jiannan Li

Stem Cell Research & Therapy (2022)

Development and verification of a three-dimensional (3D) breast cancer tumor model composed of circulating tumor cell (CTC) subsets

Muge Anil-Inevi, Pelin Sağlam-Metiner ... Sultan Gulce-Iz

Molecular Biology Reports (2020)

Proliferative Activity of Colorectal Cancer Cells with Different Levels of CD133 Expression

A. M. Gisina, Ya. S. Kim ... A. Yu. Lupatov

Bulletin of Experimental Biology and Medicine (2019)

Native-mimicking in vitro microenvironment: an elusive and seductive future for tumor modeling and tissue engineering

Girdhari Rijal & Weimin Li

Journal of Biological Engineering (2018)

IncAKHE enhances cell growth and migration in hepatocellular carcinoma via activation of NOTCH2 signaling

Guanqun Huang, Hui Jiang ... Xinke Zhou

Cell Death & Disease (2018)

PDF herunterladen
